International Journal of Mechanical, Industrial and Aerospace Sciences
ISSN: 2517-9950
Vol:8, No:6, 2014

Analysis of Cyclic Elastic-Plastic Loading of Shaft Based On Kinematic Hardening Model

Isa Ahmadi, Ramin Khamedi

Abstract**—** In this paper, the elasto-plastic and cyclic torsion of a shaft is studied using a finite element method. The Prager kinematic hardening theory of plasticity with the Ramberg and Osgood stress-strain equation is used to evaluate the cyclic loading behavior of the shaft under the torsional loading. The material of shaft is assumed to follow the non-linear strain hardening property based on the Prager model. The finite element method with C^1 continuity is developed and used for solution of the governing equations of the problem. The successive substitution iterative method is used to calculate the distribution of stresses and plastic strains in the shaft due to cyclic loads. The shear stress, effective stress, residual stress and elastic and plastic shear strain distribution are presented in the numerical results.

Keywords**—**Cyclic Loading, Finite Element Analysis, Prager Kinematic Hardening Model, Torsion of shaft.

I. Introduction

THE hysteresis behavior of structural members under cyclic loading is very important in investigation of the dynamic response of members against repeated loading, e.g. earthquake, cyclic thermo-mechanical loading of pressure vessels, dynamic cyclic loading of shaft and wind motion of structures. Generally, this kind of loading may lead to failure of the structural parts due to low cycle or high cycle fatigue of the materials through the loss of structural integrity [1]. One of the most commonly used methods in the modeling of elastic-plastic loading of structures is the incremental flow theory of plasticity which describes the yielding of the material by work hardening models, a yield surface, and a flow law. The earliest model used is the isotropic hardening model proposed by Hill [2]. Hill assumed that equal hardening occurs in all directions in yield surface and so this model considers that the plastic flow occurs in all directions. However, in cyclic loadings this model cannot predict the experimental evidence of the Bauschinger effect, which is significant due to stress reversals. To overcome this difficulty, Prager [3] in 1956 suggested the kinematic hardening model, which was later modified by Ziegler [4] in 1959. Considering a single yield surface, Prager [3] attempted to represent strain hardening by the rigid body translation of the yield surface in the stress space. Another nonlinear hardening model is Armstrong and Frederick model [5] that can predict the ratcheting response of materials in cyclic loading. Ziegler [4] assumed that the translation of the yield surface is in the direction of the vector joining the stress point on the yield surface and the center of the yield surface. In the recent years Mahbadi and Eslami [6] and [7] in 2002 and 2006 studied the cyclic loading of beams and thick vessels based on the Proger and Armstrong–Frederick kinematic hardening model. In this paper the cyclic torsion of a shaft in the elastic-plastic zone is studied using the Prager kinematic hardening model via the finite element formulation. The stress-strain and residual shear stress and strain in the shaft subjected to cyclic loading is obtained in the developed finite element code.

Isa Ahmadi is with the Mechanical Engineering Department, Faculty of Engineering, University of Zanjan, Zanjan, Iran, (phone: +94 24 3305 4058; fax: +94 42 3228 3204; e-mail: i_ahmadi@ znu.ac.ir).

Ramin Khamedi is with the Mechanical Engineering Department, Faculty of Engineering, University of Zanjan, Zanjan, Iran (e-mail: khamedi@znu.ac.ir).

II. Formulation

Consider a prismatic bar subjected to a twisting couple. One end of the bar is assumed to be fixed against rotation but not against warping. At the other end a couple T with a moment along z axis is applied. In the absence of tension and bending loads, the only nonzero strains in the bar are the shear strains ε_{xz} and ε_{yz}. In this problem, the equilibrium equations in x and y direction identically are satisfied and the equilibrium equations in z direction can be written as;

$$\frac{\partial \tau_{xz}}{\partial x}+\frac{\partial \tau_{yz}}{\partial y}=0 \tag{1}$$

Now the stress function ϕ is introduced such that

$$\tau_{xz}=\frac{\partial \phi}{\partial y},\quad \tau_{yz}=-\frac{\partial \phi}{\partial x} \tag{2}$$

By substitution of (2) in (1) the only equilibrium equation is identically satisfied. For a prismatic bar in torsion, it can be shown that the compatibility equations for infinitesimal displacement can be converted to

$$\frac{\partial \varepsilon_{yz}}{\partial x}-\frac{\partial \varepsilon_{xz}}{\partial y}=\alpha \tag{3}$$

where α is a constant. Using the elastic-plastic stress-strain relation the shear strains could be written as;

$$\begin{aligned}\varepsilon_{xz}&=1/(2G)\tau_{xz}+\varepsilon_{xz}^{p}\\ \varepsilon_{yz}&=1/(2G)\tau_{yz}+\varepsilon_{yz}^{p}\end{aligned} \tag{4}$$

where ε^p_{xz} and ε^p_{yz} are the accumulated plastic components of the total shear strain. By substituting (4) in to (3) the compatibility equations is obtained in terms of the stresses as;

$$\frac{\partial \tau_{yz}}{\partial x} - \frac{\partial \tau_{xz}}{\partial y} = 2G\alpha + g(x, y) \tag{5}$$

in which *g(x, y)* is defined as;

$$g(x, y) = 2G\left(\frac{\partial \varepsilon^p_{xz}}{\partial y} - \frac{\partial \varepsilon^p_{yz}}{\partial x}\right) \tag{6}$$

Now by substituting the stress function ϕ from (2) in to (5), the following equation will be obtained;

$$\frac{\partial^2 \phi}{\partial x^2} + \frac{\partial\, \phi}{\partial y^2} = -(2G\alpha + g(x, y)) \tag{7}$$

And ϕ=0 on the boundary of the domain. The torque acting on the section of the shaft can be obtained by;

$$T = 2\iint \phi\, dx dy \tag{8}$$

III. Finite Element Model

In this paper the finite element method is used to solve (8) with his boundary conditions. For increasing the accuracy the rectangular element with C^1 continuity is used. For this, a quadratic element with 4 node and 3 degree of freedom in each node is applied to solve the problem. This element with the natural coordinate is shown in Fig. 1. The governing equation of the problem is discretized using this finite element model.

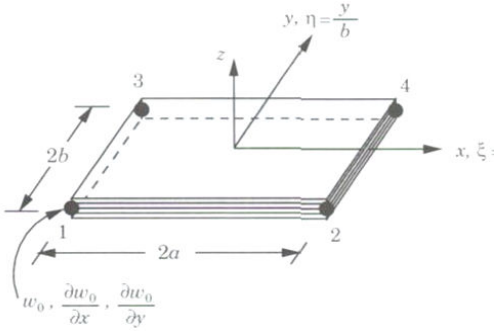

Fig. 1 The selected 4 node C^1 continuous element

The element with the length *2a* and width *2b* can be map to natural coordinate as;

$$\xi = \frac{(x - x_i)}{a} - 1, \qquad -1 \le \xi \le 1$$
$$\eta = \frac{(y - y_i)}{b} - 1, \qquad -1 \le \eta \le 1 \tag{9}$$

Using this finite element model of the stiffness matrix can be obtained as;

$$[K]^{(e)} = \int_{A(e)} [B_g]^T [D][B_g] dA =$$
$$= \int_{-1}^{1}\int_{-1}^{1} [B_l]^T [J^{-1}]^T [D][J]^{-1}[B_l] \,|J|\, d\xi d\eta \tag{10}$$

and the force vector can be obtained as;

$$\{F\}^{(e)} = -2G\theta \int_{-1}^{1}\int_{-1}^{1} |J|\, \{N_i\} d\xi d\eta \tag{11}$$

In which the Jacobean of transformation is defined as;

$$[J] = \begin{bmatrix} \frac{\partial x}{\partial \xi} & \frac{\partial y}{\partial \xi} \\ \frac{\partial x}{\partial \eta} & \frac{\partial y}{\partial \eta} \end{bmatrix} = \begin{bmatrix} a & 0 \\ 0 & b \end{bmatrix} \tag{12}$$

The details of the stiffness and force matrix are not given hear. In this study the Prager kinematic hardening model is used to model the cyclic loading and the method of successive approximation is used to evaluate the nonlinear plastic behavior of the material. In this method, the loading path is divided in to the number of increment. For each increment of load the successive approximation is used to evaluate the plastic strains. This method is described in detail in [8]. Prandtl-Reuss plastic stress-strain equation is used in this study.

IV. Results and Discussions

The cyclic loading of circular and square shaft subjected to torsion is studied in this section. In the numerical results the material is supposed to obey the Ramberg and Osgood stress-strain equation. The stress-strain equation according to Ramberg and Osgood equation can be written as [8],

$$\varepsilon = \frac{\sigma}{E} + m\left(\frac{\sigma}{E}\right)^n \tag{13}$$

where ε is the strain, σ is the stress E is the module of elasticity of the material and m and n are the material constants. The following dimensionless parameters are defined as;

$$S = \frac{\sigma_x}{\sigma_0}, \quad e = \frac{\varepsilon_x}{\varepsilon_0}, \quad e^p_x = \frac{\varepsilon^p_x}{\varepsilon_0}, \tag{14}$$

in which σ_0 is the yield stress and ε_0 is the yield strain of the material. Using the dimensionless parameters defined in (14), relations in (13) can be written as;

$$e = S + m\varepsilon_0^{n-1}(S)^n \tag{15}$$

In this study the Ramberg-Osgood parameters are chosen: $\varepsilon_0 = 0.001$, $m = 20\times10^3$, $n = 2$ and E=200GPa.

By using the following parameters the dimensionless stress-strain equation can be obtained as;

$$e = S + 20\ S^2 \tag{16}$$

In which $e=\varepsilon/\varepsilon_0$ is the dimensionless strain and $S=\sigma/\sigma_0$ is the dimensionless stress. The stress strain diagram according to (16) is shown in the Fig. 2.

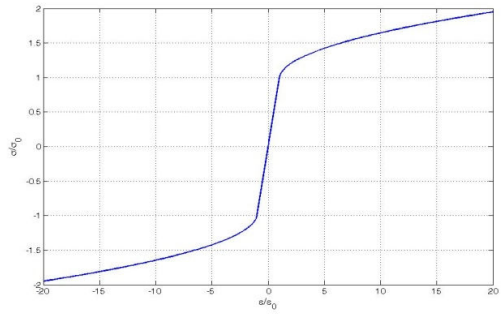

Fig. 2 The stress-strain curve of the shaft in tension and compression

A. Shaft with Circular cross-Section

First the numerical results presented for a shaft with circular cross-section. The shaft diameter is chosen $R=0.1m$. In this study the torque T which causes the first yielding and plastic strain in the shaft is called the critical torque T_{crit}. In the first example a shaft with $R=0.1\ m$ are loaded to $T=3T_{crit}$. The distribution of the dimensionless shear stress $\tau_{\theta z}/\sigma_0$ in the section of the shaft is shown in Fig. 3 and the distribution of the plastic shear strain $\varepsilon^p_{\theta z}/\varepsilon_0$ is shown in the Fig. 4. It is seen from Fig. 4 that in $r<0.25R$ the shaft is in elastic zone and $\varepsilon^p_{\theta z}=0$. For $r<0.25R$ the shaft is entered to the plastic zone. The maximum plastic shear strain in the shaft is in $r=R$ and is $\varepsilon^p_{\theta z}=2.5\varepsilon_0$.

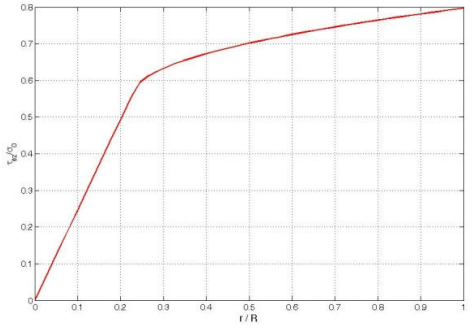

Fig. 3 Distribution of the shear stress $\tau_{\theta z}$ in the cross section of the circular shaft ($T=3T_{crit}$)

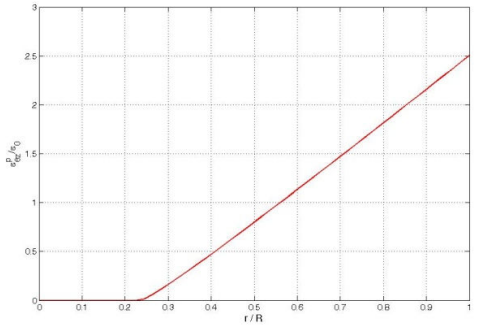

Fig. 4 Distribution of the dimensionless plastic shear strain $\varepsilon^p_{\theta z}/\varepsilon_0$ in cross-section of the shaft

Fig. 5 shows the effective stress versus effective strain diagram of a point at $r=R$ of circular shaft due to torsion. It is seen that the effective stress-effective strain diagram of the shaft coincided with the Ramberg-Osgood diagram of the material of the shaft.

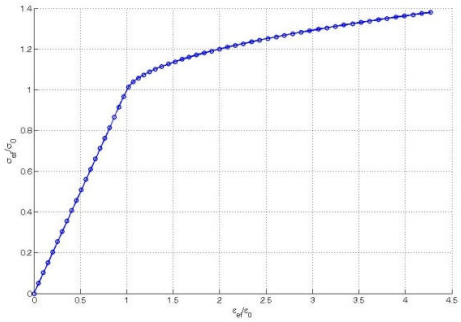

Fig. 5 Effective stress versus effective strain diagram of the material

Fig. 6 shows the dimensionless shear stress-shear strain diagram of the shaft that loaded to $T=3T_{crit}$ and unloaded to $T=0$ which is drawn for outside surface of the shaft at $r=R$. it is seen that plastic strains is occurred in the unloading of the shaft.

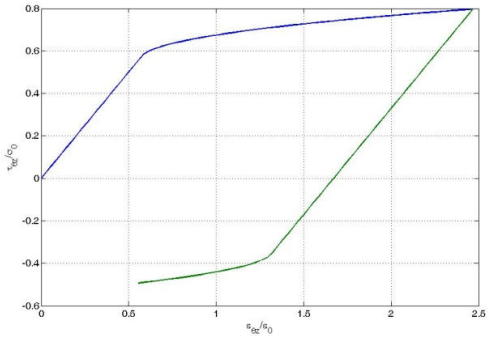

Fig. 6 Loading of circular shaft to $T=3T_{crit}$ and unloading to $T=0$

The shear stress versus shear strain diagram at outside surface of the shaft due to cyclic loading between $T=3T_{crit}$ and $T=-3T_{crit}$ is shown in Fig. 7 reversed plasticity behavior is seen after loading, unloading and reloading in Fig. 7.

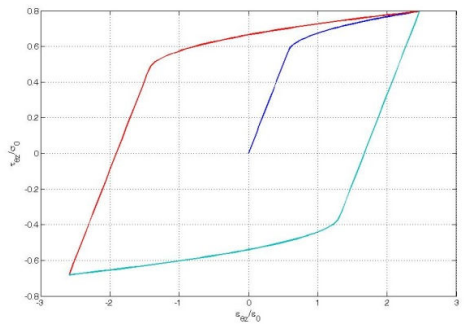

Fig. 7 Cyclic loading of circular shaft between $T=3T_{crit}$ and $T=-3T_{crit}$

B. Shaft with Square Cross-Section

In this section a shaft with square cross-section $L=W=a=0.1m$ that loaded to plastic zone are studied. The distribution of the shear stress τ_{xz} in the cross-section of the shaft for $T=2T_{crit}$ are shown in Fig. 8. Plastic zone is seen in the Fig. 8. The distribution of plastic shear strain ε^p_{xz} in the cross section of the square shaft is shown in Fig. 9.

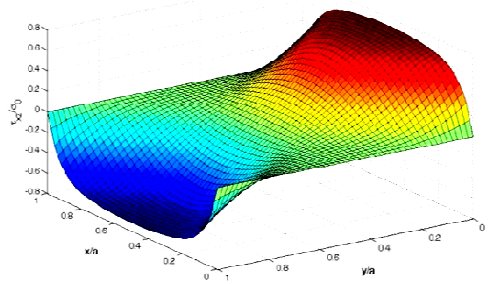

Fig. 8 Distribution of the shear stress τ_{xz} in the cross section of square shaft ($T=2T_{crit}$)

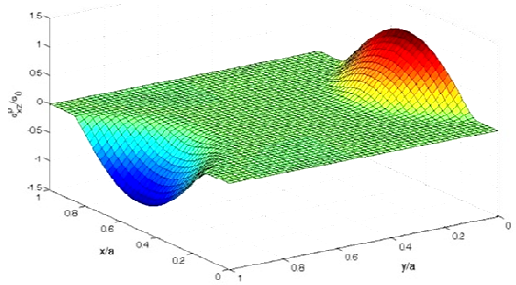

Fig. 9 Distribution of the shear strain ε^p_{xz} in the cross section of square shaft ($T=2T_{crit}$)

Fig. 10 shows the Ramberg-Osgood stress-strain curve (solid line in the figure) and the effective stress versus effective strains in the middle of the side of the square shaft ($x=a$, $y=0$) in loading to $T=3T_{crit}$ and unloading to $T=0$ (circles o).

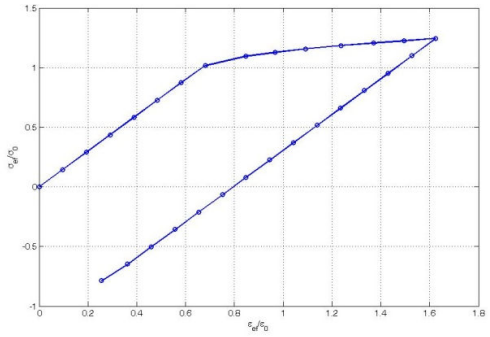

Fig. 10 Effective stress and effective stress diagram for a loading to $T=3T_{crit}$ and unloading to $T=0$

Fig. 11 shows the effective stress versus effective strain at point $x=a$ and $y=0$ in cyclic loading of the shaft between $T=2T_{Crit}$ and $T=-2T_{Crit}$. Reversed plasticity is seen in the figure for cyclic loading.

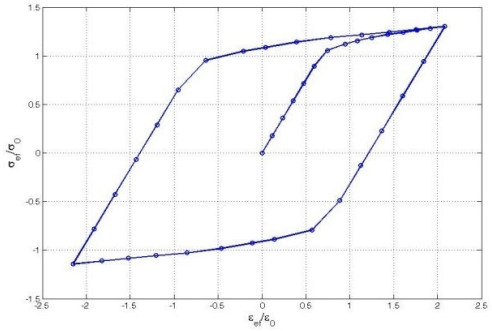

Fig. 11 Cyclic loading of square shaft between $T=2T_{Crit}$ and $T=-2T_{Crit}$

V. Conclusion

In this paper, a finite element method with C^1 continuous element is conjugated with a numerical iterative method which is quite capable and efficient to handle the analysis of the cyclic loading of structures is proposed to analysis the torsional cyclic loading of shafts. Using this method, the cyclic loading of shafts under different types of torsion is studied. The Prager kinematic hardening model is employed to model the strain hardening behavior of the material. It is concluded that the cyclic loading of shaft based on the Prager model results into reversed plasticity for all types of cyclic loadings, provided that the material strain hardening curves in tension and compression are identical.

References

[1] Sinha S., Ghosh S. "Modeling cyclic ratcheting based fatigue life of HSLA steels using crystal plasticity FEM simulation and experiments", Int J Fatigue, 28(12), 2006, pp. 1690–704

[2] Hill, R. "Mathematical Theory of Plasticity". Oxford University Press, Oxford, 1950

[3] Prager, W. "A new method of analyzing stresses and strains work-hardening plastic solids, Journal of Applied Mechanics", 1965, pp. 493–496.

[4] Ziegler H. "A modification of Prager's hardening rule", Quart. Appli. Math. 17, 1959, pp.55-65.

[5] Armstrong, PJ., Frederick, CO. "A mathematical representation of the multiaxial bauschinger effect", CEGB Report No. RD/B/N 731, 1966.
[6] Mahbadi, H., Eslami, M.R. "Cyclic Loading of Beams, Based on the Prager and Frederick-Armstrong, Kinematic hardening Model", Int. J. of Mechanical Sciences, 44, 2002, pp. 859-879.
[7] Mahbadi, H. and Eslami, M.R. "Cyclic Loading of Thick Vessels Based on the Prager and Frederick-Armstrong Kinematic Hardening Model", International Journal of Pressure Vessels and Piping, 83, 2006, pp. 409–419.
[8] Mendelson, Alexander. "Plasticity: Theory and Application" Macmillan, New York, 1968.